Journal of Statistical Physics, Vol. 73, Nos. 1/2, 1993

Numerical Analysis of a Shock-Wave Solution of the Enskog Equation Obtained via a Monte Carlo Method

Aldo Frezzotti[1] **and Carlo Sgarra**[1]

Received March 9, 1993; final May 17, 1993

In this paper a planar stationary shock-wave-like solution of the Enskog equation obtained via a Monte Carlo technique is studied; both the algorithm used to obtain the solution and the qualitative behavior of the macroscopic quantities are discussed in comparison with the corresponding solution of the Boltzmann equation.

KEY WORDS: Kinetic theory; gas dynamics; Enskog equation; dense gases; shock wave; Monte Carlo methods.

1. INTRODUCTION

In rarefied gas dynamics the Boltzmann equation seems to be a quite satisfactory tool to describe a wide class of phenomena. In 1921 Enskog[1] proposed to modify the Boltzmann equation in such a way as to describe the behavior of moderately dense gases. The equation proposed by Enskog is the following:

$$\frac{\partial F}{\partial t} + \xi \circ \nabla_x F = J_E(F, F) \tag{1}$$

where

$$\begin{aligned} J_E(F, F) = a^2 \iint & (\xi_r \circ \hat{\mathbf{k}})\, H(\xi_r \circ \hat{\mathbf{k}}) \\ & \times \left[Y\left(n\left(\mathbf{x} + \frac{a}{2}\hat{\mathbf{k}}\right)\right) F(\xi^*, \mathbf{x}, t)\, F(\xi_1^*, \mathbf{x} + a\hat{\mathbf{k}}, t) \right. \\ & - Y\left(n\left(\mathbf{x} - \frac{a}{2}\hat{\mathbf{k}}\right)\right) \\ & \left. \times F(\xi, \mathbf{x}, t)\, F(\xi_1, \mathbf{x} - a\hat{\mathbf{k}}, t) \right] d\xi_1\, d\hat{\mathbf{k}} \end{aligned} \tag{2}$$

[1] Department of Mathematics, Politecnico di Milano, 32-20133 Milan, Italy.

0022-4715/93/1000-0193$07.00/0

In Eq. (2), a is the diameter of the molecules (assumed to behave like hard spheres), ξ_r is the relative speed of the centers, $\hat{\mathbf{k}}$ is the unit vector of the line joining the centers of the molecules, H is the Heaviside step function, and the Y factor is a function of the space and time variables through the density $n(\mathbf{x}, t)$ evaluated where the molecules come into contact. As clearly appears from Eq. (1), the Enskog equation attempts a description of the behavior of dense gases by retaining the binary structure of the Boltzmann collision integral. However, the molecules are no longer considered dimensionless points and the collision partners occupy different positions. Moreover, the factor Y brings into the collision rate the effects of mutual shielding and of the reduction of volume available for molecular motion. In the present work, the Y factor originally proposed by Enskog has been adopted.[2, 3]

Although the Boltzmann equation has received much more attention, in recent years interest in the Enskog equation has grown and interesting results are available for the problems of existence, uniqueness, and asymptotic behavior of the solutions.[4, 5] However, to our knowledge, no explicit solution is known, either analytical or numerical. Therefore, dense gases have been studied by other theoretical tools, such as Navier–Stokes equations or computer experiments on molecular dynamics.[6]

In this paper the classical problem of the propagation of a shock wave is studied numerically within the framework of the Enskog equation. The adopted numerical method is an extension of a Monte Carlo technique already used to obtain solutions of the Boltzmann equation. In the next section the problem of conservation equations and the role of the Rankine–Hugoniot conditions are briefly discussed; in Section 3 the numerical technique is described, while the numerical results are described and discussed in Section 4.

2. BASIC EQUATIONS AND THE RANKINE–HUGONIOT RELATIONS

As anticipated in the previous section, in the present paper the propagation of a plane shock wave in a dense gas is studied. Attention is focused on the calculation of the fully formed shock profile, which appears stationary to an observer moving with the shock front. Accordingly, numerical solutions of the following one-dimensional steady equation are sought:

$$\xi_x \frac{\partial F}{\partial x} = J_E(F, F) \tag{3}$$

The boundary conditions for Eq. (3) are

$$\lim_{x \Rightarrow -\infty} F(x, \xi) = \frac{n_1}{(2\pi RT_1)^{3/2}} \exp\left[-\frac{(\xi - U_1)^2}{2RT_1} \right] \tag{4a}$$

$$\lim_{x \Rightarrow +\infty} F(x, \xi) = \frac{n_2}{(2\pi RT_2)^{3/2}} \exp\left[-\frac{(\xi - U_2)^2}{2RT_2} \right] \tag{4b}$$

since it is assumed that far from the shock, equilibrium conditions exist. In Eqs. (4) n_1, U_1, T_1 and n_2, U_2, T_2 are the density, bulk velocity, and temperature, respectively, of the upstream and downstream equilibrium distribution, and R is the gas constant. The parameters of the downstream and upstream equilibrium states are connected by the following modified Rankine–Hugoniot relationships:

$$n_1 U_1 = n_2 U_2 \tag{5a}$$

$$n_1[U_1^2 + RT_1(1 + bYn_1)] = n_2[U_2^2 + RT_2(1 + bYn_2)] \tag{5b}$$

$$[U_1^2 + RT_1(5 + 2bYn_1)] = [U_2^2 + RT_2(5 + 2bYn_2)] \tag{5c}$$

since the upstream and downstream fluxes of mass momentum and energy must be equal. The quantities Y and b appearing in Eqs. (5) are defined as

$$Y(n) = \frac{1 + (11/8)\, bn}{1 - 2bn} \tag{6}$$

where $b = (2/3)\, \pi a^3$. In complete analogy with the classical case, the problem of solving Eqs. (5) can be reduced to determining the intersection of a straight line (the Raleigh straight line) with a more complex curve (the Hugoniot hyperbola in the classical case). The abscissa of the intersection point is determined numerically and gives the ratio n_1/n_2.

In investigating the planar shock-wave behavior of a dense gas it is tempting to use the Mott–Smith ansatz[7] in a fashion analogous to the Boltzmann case. The success of the Mott–Smith approach is crucially related to the linearity of the ansatz, which allows the automatic conservation of mass, momentum, and energy everywhere in the flow field once the Rankine–Hugoniot relationships hold. The unknown amplitude function may be therefore determined by writing a balance equation for a nonconserved quantity. In a recent paper, Orlov[8] presented an application of the Mott–Smith method to a kinetic equation derived from the Enskog equation assuming that the parameter na^3 (the product of a characteristic number density times the cube of the molecular diameter) is small. Unfortunately, in this case the Mott–Smith distribution function can no

longer ensure the conservation of momentum and energy fluxes throughout the whole flow field. In fact, the nonlocal collision integral brings into the fluxes a term of the order of na^3 which is quadratic in the amplitude appearing in the ansatz. The coefficient of the quadratic term does not vanish when Eqs. (5) hold, and the fluxes cannot be constant.

3. DESCRIPTION OF THE NUMERICAL METHOD

The numerical method used to calculate approximate solutions of Eq. (1) is the natural extension of the so-called "direct method" proposed in 1959 by Nordsieck[9] to solve the Boltzmann equation. The method is based on a finite difference scheme combined with Monte Carlo techniques to evaluate the collision integral. Over the years, the original Nordsieck algorithm has been modified and improved by several authors who applied it to calculate one-, two-, and three-dimensional solutions of the Boltzmann equation for a monatomic gas[10, 11] and one-dimensional flows of mixtures and polyatomic gases.[17] As far as the Boltzmann equation is concerned, the direct method is not as popular as Bird's direct simulation Monte Carlo method (DSMC) and its various "dialects." The former method was less succesfull because of its greater demand of computer memory, which makes it impractical in multidimensional problems, i.e., in most of the practical applications of rarefied gas dynamics. The situation is more favorable in one-dimensional problems, where the memory demand is smaller. Furthermore, the algorithm is ideally suited for vector and/or parallel processing.[17] Since no analog DSMC or particle scheme has yet been proposed for the Enskog equation, the direct method suggests itself as a consistent numerical scheme that can be used as a starting point.

The numerical algorithm adopted in the present work is based on the normalized form of the Enskog equation:

$$\frac{\partial F}{\partial t}+\xi_x\frac{\partial F}{\partial x}=J_{\mathrm{E}}(F,F)=G_{\mathrm{E}}(x,\xi\,|\,t)-\nu_{\mathrm{E}}(x,\xi\,|\,t)\,F(x,\xi\,|\,t) \tag{7}$$

where

$$G_{\mathrm{E}}(x,\xi\,|\,t)=\frac{1}{\sqrt{2}\,\pi Y_1}\int d\xi_1\int d\hat{\mathbf{k}}\;Y\left[n\left(x+\frac{E}{2}k_x\right)\right]$$
$$\times F(x,\xi^*)\,F(x+Ek_x,\xi_1^*)(\xi_r\circ\hat{\mathbf{k}})\,H(\xi_r\circ\hat{\mathbf{k}}) \tag{8a}$$

$$\nu_{\mathrm{E}}(x,\xi\,|\,t)=\frac{1}{\sqrt{2}\,\pi Y_1}\int d\xi_1\int d\hat{\mathbf{k}}\;Y\left[n\left(x-\frac{E}{2}k_x\right)\right]$$
$$\times F(x-Ek_x,\xi_1)(\xi_r\circ\hat{\mathbf{k}})\,H(\xi_r\circ\hat{\mathbf{k}}) \tag{8b}$$

In the above equations F is the distribution function normalized to $n_1/(RT_1)^{3/2}$, where n_1 and T_1 are reference values of the number density and temperature, respectively. The molecular velocity ξ is normalized to $(RT_1)^{1/2}$, the spatial coordinate x is normalized to the upstream mean free path $\lambda_1 = 1/[\sqrt{2}\,\pi a^2 n_1 Y(n_1)]$, while the time is normalized to $\tau = \lambda_1/(RT_1)^{1/2}$. The dimensionless parameter E is defined as the ratio of the molecular diameter to the reference mean free path λ_1 and is related to the parameter $N_1 = (4\pi a^3/3)n_1$ by the simple relationship

$$E = Y_1 \sqrt{2}\, \tfrac{3}{4} N_1 \tag{9}$$

where

$$Y_1 = \frac{1 - 11/16 N_1}{1 - N_1} \tag{10}$$

The first step toward the construction of the algorithm is the choice of a proper discretization of the distribution function in the physical and velocity spaces. In this work the region occupied by the standing shock wave (an interval on the x axis centered about the origin) has been divided into a number of cells of the same size, and the distribution function assumed to be spatially homogeneous within each cell. A similar procedure has been adopted to represent the distribution function in the velocity domain consisting of a finite cylinder. The domain has to be chosen wide enough to contain the significant part of the distribution function at any stage of the calculations. In the problem considered here computer storage is saved by taking advantage of the symmetry of F, which depends on the velocity through the arguments ξ_x and $\xi_\perp = (\xi_y^2 + \xi_z^2)^{1/2}$.

Accordingly, a regular net of nodes $(\xi_x, \xi_\perp)$ is arranged into the rectangular region whose rotation about the x axis generates the cylindrical velocity domain. It is assumed that the distribution function is constant within each ringlike cell of center ξ_x and mean radius $\xi_\perp$. The discretized solution of the finite difference analog of Eq. (7) is advanced from one time level to the next by time-splitting the evolution operator. First molecules move freely trough the spatial grid according to the equation

$$\frac{\partial F(\xi, x, t)}{\partial t} + \xi_x \frac{\partial F(\xi, x, t)}{\partial x} = 0 \tag{11}$$

Then the collisional process takes place in each cell of the spatial grid according to the equation

$$\frac{\partial F(\xi, x, t)}{\partial t} = J_E(\xi, x, t) \tag{12}$$

The time-splitting method described above closely patterns the procedure first proposed by Bird[12] and used in particle schemes, in which the free molecular motion and the intermolecular collisions are two independent stages of the algorithm that update the particle position and velocity. It is worth noticing that Eq. (12) does not describe a homogeneous relaxation, since the evaluation of the collision integral $J_E(\xi, x, t)$ involves the distribution function in nearby cells.

Within the framework of the present finite difference method the first step is performed by a simple first-order explicit upwind conservative scheme.

As far as the collisional step is concerned, at each spatial location x_i, Eq. (12) is integrated over the cell $\vartheta(l, m)$ of the velocity space:

$$\frac{d}{dt} N(l, m, i \mid t) = \int_{\vartheta(l,m)} d\xi \, J_E(\xi, x_i, t) \equiv J_E(l, m, i \mid t) \tag{13}$$

where

$$N(l, m, i \mid t) = \int_{\vartheta(l,m)} F(\xi, x_i, t) \, d\xi = \Delta v(l, m) \, F(l, m, i \mid t) \tag{14}$$

In Eqs. (13) and (14), $N(l, m, i \mid t)$ represents the expected number of particles in the cell centered around the velocity node $\xi(l, m)$, while $\Delta v(l, m)$ and $F(l, m, i \mid t)$ are the cell volume and the mean value of $F(\xi, x_i, t)$ in the cell, respectively.

The integral appearing in Eq. (13) can be transformed into an integral extended to the whole velocity domain $\mathscr{V}$ by introducing $\chi_{l,m}(\xi)$, the characteristic function of the cell $\vartheta(l, m)$:

$$\frac{d}{dt} N(l, m, i \mid t) = \int_{\mathscr{V}} \chi_{l,m}(\xi) \, J_E(\xi, x_i, t) \, d\xi \tag{15}$$

Now, taking into account the expression of $J_E(\xi, x, t)$ and making use of some fundamental properties of the collision integral, Eq. (15) can be written in the following form:

$$\frac{d}{dt} N(l, m, i \mid t) = \tfrac{1}{2} \int_{\mathscr{V}} [\chi_{l,m}(\xi) - \chi_{l,m}(\xi^*)] \, J_E(\xi, x_i, t) \, d\xi \tag{16}$$

The eightfold integral at the right-hand side of the above equation is evaluated by a Monte Carlo quadrature method,[16] since a regular method would be computationally too expensive. The procedure that carries out the evaluation of the collision integral in the ith spatial cell can be roughly described as follows:

(a) A sequence of N_{Test} "collision partners" ξ, ξ_1 and collision parameters $\mathbf{k}$ is generated, the velocity ξ and ξ_1 being uniformly distributed in $\mathscr{V}$ and the vectors $\mathbf{k}$ uniformly distributed on the unit sphere.

(b) The postcollision velocity vectors are calculated from

$$\xi^* = \xi + (\hat{\mathbf{k}} \cdot \xi_r)\xi_r$$
$$\xi_1^* = \xi_1 - (\hat{\mathbf{k}} \cdot \xi_r)\xi_r$$

(c) As indicated in Eq. (16), each collision is used to update the value of the collision integral in the cells of the velocity space containing ξ and ξ^*. The same collision also contributes to the calculation in the cells containing ξ_1 and ξ_1^* when the roles of ξ and ξ_1 are exchanged.

The three steps sketched above are repeated at each spatial location keeping the same sample of N_{Test} collision. The sample is renewed at the beginning of each time step.

Once the collision integral has been evaluated, the solution is advanced from the qth time level to the next according to the explicit scheme

$$F^{(q+1)} = F^{(q)} + J_{\text{E}}^{(q)} \Delta t \tag{17}$$

As is well known, the application of the technique described above to the numerical solution of the Boltzmann equation leads to a scheme in which mass, momentum, and energy are not exactly conserved. The numerical errors are usually small, but have the unpleasant feature of accumulating during the time evolution of the distribution function. There are several error sources, but the most fundamental one is the use of a discretized velocity space. Although the procedure described above does practically eliminate the mass error, it is only able to reduce the error associated with momentum and energy. In the case of the Boltzmann equation, Aristov and Tcheremissine[15] proposed a correction method to overcome the difficulty. At each time step the distribution function is corrected in the following way:

$$\tilde{F}^{(q+1)}(\xi) = F^{(q+1)}(\xi)(1 + A + \mathbf{B} \circ \xi + C\xi^2) \tag{18}$$

In Eq. (18) $F^{(q+1)}(\xi)$ is the distribution function computed from Eq. (17). A corrected distribution function $\tilde{F}^{(q+1)}(\xi)$ is computed multiplying $F^{(q+1)}(\xi)$ by the polynomial $P(\xi) = 1 + A + \mathbf{B} \circ \xi + C\xi^2$. The constants A, $\mathbf{B}$, and C are determined from the conditions:

$$\int \psi(\xi)\, \tilde{F}^{(q+1)}(\xi)\, d\xi = \int \psi(\xi)\, F^{(q)}(\xi)\, d\xi, \qquad \psi(\xi) = 1,\ \xi,\ \xi^2 \tag{19}$$

It is worth mentioning that the correction method outlined above, although consistent[15] (it does not destroy the consistency of the finite difference scheme), has no clear theoretical ground. Its validity should be checked in any situation and the grid in the velocity space should be refined until no changes in the final results is observed.

A similar correction step has been added to the algorithm that computes the numerical solution of the Enskog equation. Since momentum and energy are not locally conserved by the Enskog collision term, the coefficients of the correction polynomial cannot be obtained on the ground of Eqs. (19). Two of them have to be replaced by the momentum and energy collisional balance:

$$\int \xi_x \tilde{F}^{(q+1)}(\xi)\, d\xi = \int \xi_x F^{(q)}(\xi)\, d\xi + \dot{\mathcal{M}}\, \Delta t \tag{20}$$

$$\int \xi^2 \tilde{F}^{(q+1)}(\xi)\, d\xi = \int \xi^2 F^{(q)}(\xi)\, d\xi + \dot{\mathscr{E}}\, \Delta t \tag{21}$$

where

$$\begin{pmatrix} \dot{\mathcal{M}} \\ \dot{\mathscr{E}} \end{pmatrix} = \int_{\mathscr{V}} \begin{pmatrix} \xi_x \\ \xi^2 \end{pmatrix} J_E(\xi, x, t)\, d\xi \tag{22}$$

Before describing and discussing the numerical results a few comments are in order. It should be noticed that the choice of a time explicit scheme to update F could be dangerous because it might lead to negative values of the distribution function. The negative values which are sometime observed are limited to the regions where the absolute value of F is extremely small. Accordingly, negative value are simply set equal to zero.

The effects of the truncation are easily monitored because cutting an excessively large part of F would be manifest through a large mass error. Although the procedure might look less reassuring than the use of a "safe" implicit scheme, some numerical tests show that an implicit scheme needs larger correction coefficients and finally leads to slightly larger shocks.

4. DESCRIPTION OF THE NUMERICAL RESULTS

The numerical procedure described above was used to study the propagation of shock waves in a dense gas at relatively low Mach number. Each computation started with the gas filling the half-space $x < 0$ in the upstream equilibrium condition and the half-space $x > 0$ in the downstream equilibrium condition as given by the Rankine–Hugoniot relationships. Computational parameters such as grid size, time step, and collision num-

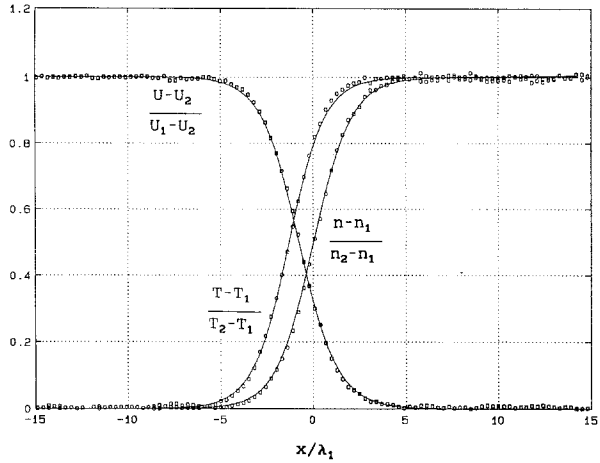

Fig. 1. Comparison of DSMC results (circles) and direct method calculations (solid lines). Mach number = 2, $E = 0$ (Boltzmann gas).

ber were varied until no appreciable changes in the solution were observed. The first series of calculations was aimed at checking the ability of the computer program to reproduce DSMC shock results in the limit case $E = 0$. In Fig. 1 the shock profiles in a hard-sphere gas obtained by the authors using Koura's null-collision DSMC[14] are compared with the corresponding results obtained from the direct method. The agreement between the two methods is rather good, although a closer examination indicates that DSMC produced slightly steeper shock profiles. Shock profiles in a dense

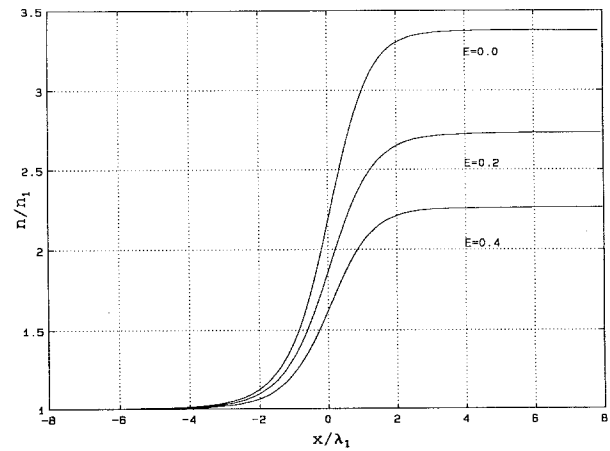

Fig. 2. Normalized density profiles. $M_B = 4$.

gas were then calculated for values of the parameter E in the range $[0, 0.4]$. For each value of E different solutions were obtained by varying the parameter $M_B = U_1/(\gamma RT_1)^{1/2}$ ($\gamma = 5/3$) in the range $(2, 4)$. It should be noticed that M_B is not the effective upstream Mach number, because the adiabatic speed of sound depends on E, too. Examples of density and temperature profiles are displayed in Figs. 2 and 3. The calculations were performed setting $M_B = 4$ and changing E. As clearly appears from Fig. 2, the density jump across the shock is reduced when E increases. This effect

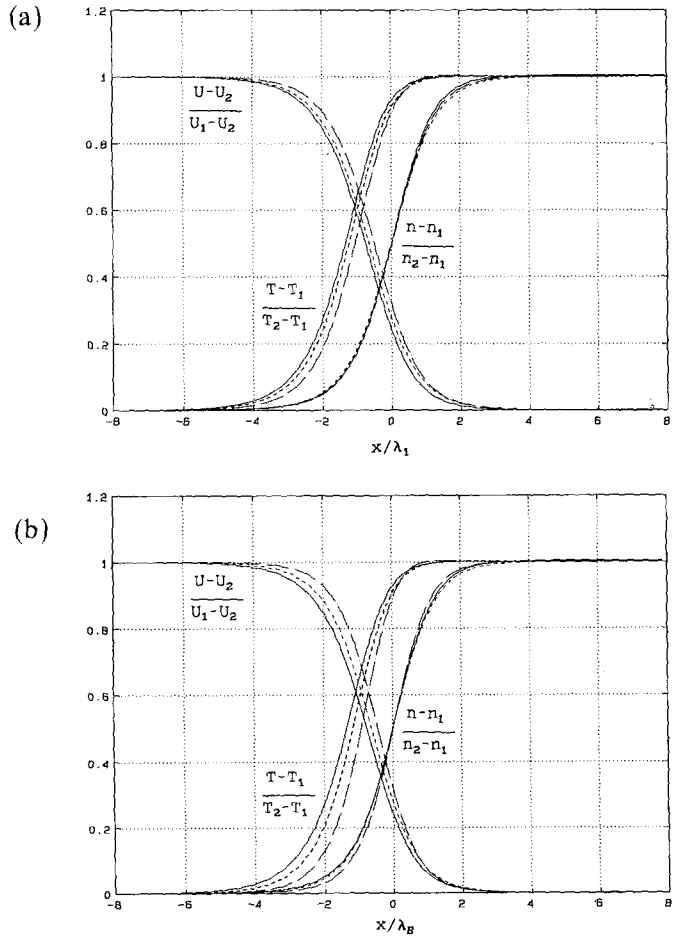

Fig. 3. (a) Effects of the parameter E on normalized shock profiles. $M_B = 4$. Solid lines, $E = 0$. Dashed lines, $E = 0.2$. Dashed-dotted lines, $E = 0.4$. (b) As in (a), but with the spatial coordinate x normalized to λ_B.

is due to the additional terms in the Rankine–Hugoniot relationships. To help comparing shock profiles in different conditions, normalized density, temperature, and velocity profiles are shown in Fig. 3a, each quantity being normalized to its own variation across the shock region. The normalized density profiles show little variations and the parameter E seems to affect mainly the lag between the temperature and density rise. This effect is more evident in Fig. 3b, where the same normalized quantities are plotted against the spatial coordinate normalized to $\lambda_B = 1/(\sqrt{2}\,\pi a^2 n_1)$, which does not depend on E. The distinctive features of the Enskog collision term are more readily appreciated from the curves displayed in Fig. 4a, where the functions $\dot{\mathcal{M}}(x)$ and $\dot{\mathcal{E}}(x)$ are plotted. These two functions give the

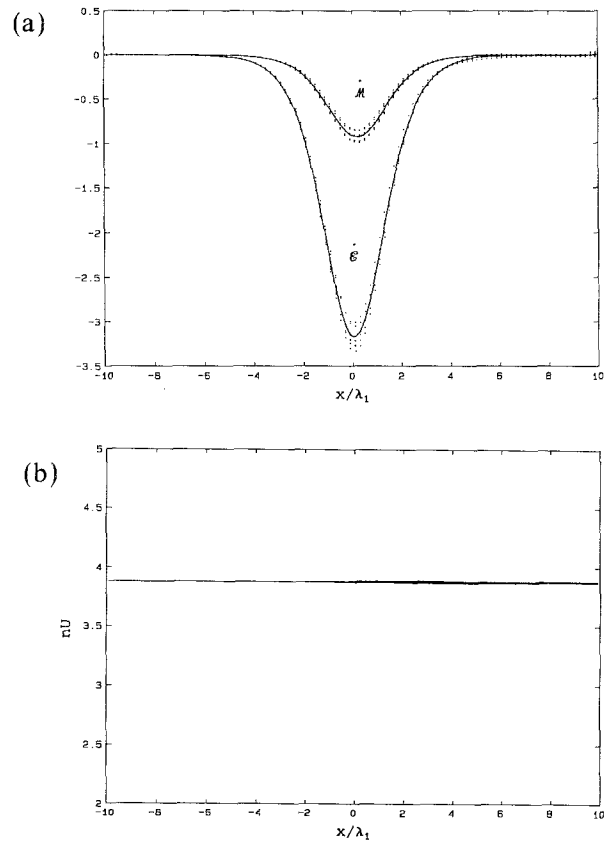

Fig. 4. (a) Profiles of the collisional rate of change of momentum ($\dot{\mathcal{M}}$) and energy ($\dot{\mathcal{E}}$). $M_B = 3.5$, $E = 0.4$. Dotted lines: instantaneous profiles. Solid lines: time-averaged curves. (b) Mass flux profiles. $M_B = 3.5$, $E = 0.4$.

normalized rate of change of momentum and energy due to the nonlocal character of the collision process. Each of the two groups of curves displayed in Fig. 4a was obtained by superposing data collected at relatively long time intervals after the onset of a steady shock profile. Owing to the statistical nature of the computational method, the data exhibit variations in time. However, the time-averaged curves (represented by the solid line in Fig. 4a satisfy the following relationships:

$$\left[\int \xi_x \begin{pmatrix} \xi_x \\ \xi^2 \end{pmatrix} F(\xi, x)\, d\xi\right]_{-\infty}^{+\infty} = \int_{-\infty}^{+\infty} \begin{pmatrix} \dot{M}(x) \\ \dot{\mathscr{E}}(x) \end{pmatrix} dx \tag{23}$$

to less than 1% of the exact value. Examples of computed mass flux profiles are shown in Fig. 4b. Again, the graph was obtained by superposing samples of the mass flux profiles collected for a long time period after the onset of the steady state. It can be noticed that very small differences exist among the individual samples, each of them being fairly constant.

The results of the computations are summarized in Fig. 5, where the reciprocal shock thickness δ^{-1} is plotted as a function of the Mach number for various values of the parameter E. The reciprocal shock thickness is defined as the maximum value of the normalized density gradient:

$$\delta^{-1} = \frac{1}{n_2 - n_1} \left(\frac{dn}{dx}\right)_{\text{Max}} \tag{24}$$

The data displayed in Fig. 5a have been obtained by a time average of the maximum density gradient, which decreases very rapidly toward its final value as the initial discontinuity dies out. The time averaging is necessary to suppress the unavoidable oscillations due to the Monte Carlo procedure. It is worth mentioning that the amplitude of such oscillations was about 3% of the mean value in the worst case.

At lower Mach numbers the curves are very close and differ very little from the Mott–Smith curve. As the Mach number grows, the curve corresponding to $E = 0.4$ goes above the Boltzmann curve ($E = 0$), while the curve corresponding to $E = 0.2$, although very close to the Boltzmann case, remains slightly below it. The nonmonotonic behavior of the reciprocal shock thickness is even more evident upon plotting δ^{-1} against M_B, as in Fig. 5b, where the crossing of the curves is evident.

A qualitative explanation of this behavior can be attempted assuming that the shock thickness is of the order of λ_{12}, the mean free path of the molecules entering the high-density, low-speed region from the low-density, high-speed region. Neglecting the details of the distribution function, an approximate value for λ_{12} can be given by the following expression[18]:

$$\lambda_{12} \approx \frac{U_1}{U_1 - U_2} \frac{1}{\sqrt{2}\, \pi a^2 n_2\, Y(n_2)} \tag{25}$$

Therefore, an approximate value of the normalized shock thickness is given by

$$\delta \approx \frac{\lambda_{12}}{\lambda_E} = \frac{U_1}{U_1 - U_2} \frac{n_1 Y(n_1)}{n_2 Y(n_2)} \tag{26}$$

Now it can be easily checked that if M_B is fixed and E is varied, the factor $n_1 Y(n_1)/n_2 Y(n_2)$, the high-Mach-number limit of expression (26), exhibits a maximum around $E = 0.2$ if M_B is greater than 2.5. If the additional term $U_1/(U_1 - U_2)$ is taken into account, maxima are also found, but for M_B greater than 4. The assumptions used to obtain Eq. (25) are certainly more justified at high Mach number; nevertheless it is reassuring to see that the expression (26) qualitatively reproduces the behavior of the data shown in Fig. 5a.

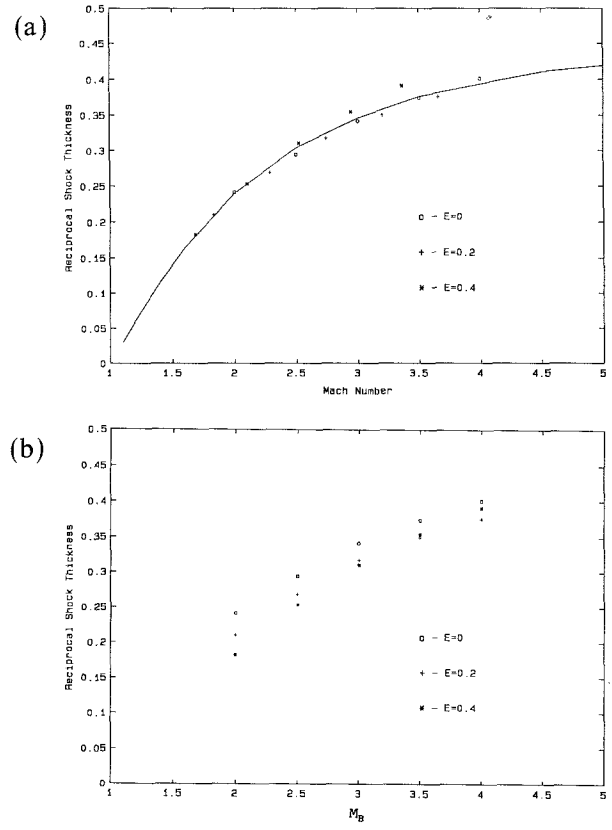

Fig. 5. (a) Reciprocal shock thickness as a function of the Mach number and E. Circles, $E = 0$; crosses, $E = 0.2$; asterisks, $E = 0.4$. Solid line, Mott–Smith ξ^2 curve for hard-sphere potential. (b) Reciprocal shock thickness as a function of the M_B and E. Circles, $E = 0$; crosses, $E = 0.2$; asterisks, $E = 0.4$.

5. CONCLUDING REMARKS

In this paper the behavior of a stationary shock wave in a dense gas has been investigated in a narrow region of the plane (M, E). Further progress in establishing the validity of the Enskog equation is essentially related to the enhancement of the efficiency of the numerical method. At present a particle scheme for the Enskog equation is being developed following the lines of Nambu's[13] scheme modified by a majorant collision frequency method.[14] The development of an alternative method will also provide an independent check of the solutions presented here.

It is worth mentioning that the Y factor appearing in the Enskog equation, for which an approximate expression has been assumed according to the classical treatments, can be evaluated in a more refined way as a pair correlation function by a suitable cluster expansion. The resulting equation is called the revised Enskog equation and the transport coefficients given by this modified version of the Enskog equation have been proved to satisfy the reciprocity relations provided by the irreversible thermodynamics[19] and an H-theorem has been proved for its solutions.[20] This could be another research line along which an improvement of the present results could be made.

An approach to the dynamics of dense gases based on the Enskog equation is intermediate between the "exact" molecular dynamics method (MD) and the hydrodynamic approach based on the Navier–Stokes equations (NSE). Hence, a comparison of the present results with those obtained by MD and NSE would be very interesting. The comparison with the hydrodynamic approach seems particularly promising in the light of the ideal gas results by Fiscko and Chapman[21] on the Burnett and super-Burnett equations on one hand and by Holian *et al.*[22] on the other. In particular the latter have shown that Navier–Stokes equations can compete with MD in describing dense fluids[6] and, more recently, that the discrepancies between the NSE and the microscopic approach can be further reduced by a suitable modification of NSE.[23] In the case of a dense gas, to our knowledge, only a linearized version of the Burnett equations has been produced.[24]

ACKNOWLEDGMENTS

The authors thank Prof. C. Cercignani for bringing Orlov's paper to their attention and for helpful discussions on the content of Section 2.

REFERENCES

1. D. Enskog, *Kinetische Theorie* (Svenska Akad., 63, 1921).
2. S. Chapman and T. G. Cowling, *The Mathematical Theory of Nonuniform Gases* (Cambridge University Press, Cambridge, 1960).
3. P. Resibois and M. De Leener, *Classical Kinetic Theory of Fluids* (Wiley, London, 1977).
4. N. Bellomo, M. Lachowicz, J. Polewczac, and G. Toscani, *Mathematical Topics in Nonlinear Kinetic Theory II: The Enskog Equation* (World Scientific, Singapore, 1991).
5. L. Arkeryd and C. Cercignani, Global existence in L^1 for the Enskog equation and convergence of the solutions to solutions of the Boltzmann equation, *J. Stat. Phys.* **59**:845–867 (1990).
6. B. L. Holian, W. G. Hoover, B. Moran, and G. K. Straub, Shock-wave structure via nonequilibrium molecular dynamics and Navier–Stokes continuum mechanics, *Phys. Rev.* **22A**:2798–2808 (1980).
7. H. M. Mott-Smith, The solution of the Boltzmann equation for a shock-wave, *Phys. Rev.* **82**:885–900 (1951).
8. A. V. Orlov, Extension of the Mott-Smith method to denser gases, *Phys. Fluids A* **4**(8):1856–1858 (1992).
9. A. Nordsieck and B. Hicks, Monte Carlo evaluation of the Boltzmann collision integral, in *Rarefied Gas Dynamics*, Vol. 2, C. L. Brundin, ed. (Academic Press, New York, 1967, pp. 695–710.
10. F. G. Tcheremissine, Fast solutions of the Boltzmann equation, in *Rarefied Gas Dynamics*, Vol. 1, A. E. Beylich, ed. (VCH, Aachen, 1991), pp. 273–284.
11. V. V. Aristov, Development of the regular method of the Boltzmann equation, in *Rarefied Gas Dynamics*, Vol. 1, A. E. Beylich, ed. (VCH, Aachen, 1991), pp. 879–885.
12. G. A. Bird, *Molecular Gas Dynamics* (Clarendon Press, Oxford, 1976).
13. K. Nambu, Theoretical basis of the direct simulation Monte Carlo method, in *Rarefied Gas Dynamics*, Vol. 2, V. Boffi and C. Cercignani, eds. (Teubner, Stuttgart, 1986), pp. 379–383.
14. K. Koura, Null collision technique in the direct simulation Monte-Carlo method, *Phys. Fluids* **29**:3509–3511 (1986).
15. V. V. Aristov and F. G. Tcheremissine, The conservative splitting method for solving the Boltzmann equation, *USSR Comp. Math. Phys.* **20**:208 (1980).
16. M. H. Kalos and P. A. Whitlock, *Monte Carlo Methods* (Wiley, New York, 1986).
17. A. Frezzotti and R. Pavani, Direct numerical solution of the Boltzmann equation for a relaxation problem of a binary mixture, *Meccanica* **24**:139 (1989).
18. M. N. Kogan, *Rarefied Gas Dynamics* (Plenum Press, New York, 1969).
19. H. Van Beijeren and M. H. Ernst, The modified Enskog equation, *Physica* **68**:437–456 (1973).
20. P. Resibois, H-theorem for the (modified) nonlinear Enskog equation, *J. Stat. Phys.* **19**:593–609 (1978).
21. K. A. Fiscko and D. R. Chapman, Comparison of Burnett, Super-Burnett and Monte Carlo solutions for hypersonic shock structure, in *Rarefied Gas Dynamics*, Vol. 1, E. P. Muntz, D. P. Weaver, and D. H. Campbell, eds. (AIAA, Pasadena, California, 1988), pp. 374–395.
22. E. Salomons and M. Mareschal, Usefulness of the Burnett description of strong shock waves, *Phys. Rev. Lett.* **69**(2):269–272 (1992).
23. B. L. Holian, C. W. Patterson, M. Mareschal, and E. Salomons, Modeling shock waves in an ideal gas: Going beyond the Navier–Stokes level, *Phys. Rev. E* **47**(1):R24–27 (1993).
24. W. Marques and G. M. Kremer, On Enskog's dense gas theory. II. The linearized Burnett equations for monatomic gases, *Rev. Bras. Fis.* **21**(3):402–417 (1991).